

# RSC Advances



This is an *Accepted Manuscript*, which has been through the Royal Society of Chemistry peer review process and has been accepted for publication.

*Accepted Manuscripts* are published online shortly after acceptance, before technical editing, formatting and proof reading. Using this free service, authors can make their results available to the community, in citable form, before we publish the edited article. This *Accepted Manuscript* will be replaced by the edited, formatted and paginated article as soon as this is available.

You can find more information about *Accepted Manuscripts* in the [Information for Authors](#).

Please note that technical editing may introduce minor changes to the text and/or graphics, which may alter content. The journal's standard [Terms & Conditions](#) and the [Ethical guidelines](#) still apply. In no event shall the Royal Society of Chemistry be held responsible for any errors or omissions in this *Accepted Manuscript* or any consequences arising from the use of any information it contains.



Journal Name

ARTICLE

## *n*-Butyraldehyde Self-Condensation Catalyzed by Ce-Modified $\gamma$ - $\text{Al}_2\text{O}_3$

Chao Xiong, Ning Liang, Hualiang An, Xinqiang Zhao\*, Yanji Wang

Received 00th January 20xx,  
Accepted 00th January 20xx

DOI: 10.1039/x0xx00000x

www.rsc.org/

Self-condensation of *n*-butyraldehyde is one of the important processes for the industrial production of 2-ethylhexanol. The catalytic performance of some solid acids such as  $\gamma$ - $\text{Al}_2\text{O}_3$  and molecular sieves for the self-condensation of *n*-butyraldehyde was investigated and the results showed that  $\gamma$ - $\text{Al}_2\text{O}_3$  was the best one. Then the effect of preparation conditions on the catalytic performance of  $\gamma$ - $\text{Al}_2\text{O}_3$  and the effect of reaction conditions on the self-condensation of *n*-butyraldehyde were discussed. In order to improve the catalytic performance,  $\gamma$ - $\text{Al}_2\text{O}_3$  was modified by different substances and Ce- $\text{Al}_2\text{O}_3$  was found to show the best catalytic performance; the conversion of *n*-butyraldehyde and the yield of 2-ethyl-2-hexenal could reach 93.8% and 88.6%, respectively. Moreover, Ce- $\text{Al}_2\text{O}_3$  catalyst had excellent reusability. The XPS analysis of Ce3d demonstrated that the valence state of cerium affected the catalytic performance of Ce- $\text{Al}_2\text{O}_3$  to some extent but not predominantly. Instead the acid-base property of Ce- $\text{Al}_2\text{O}_3$  played a dominant role in the catalytic performance. The reaction components formed over Ce- $\text{Al}_2\text{O}_3$  catalyst were identified by GC-MS and then some side-reactions were speculated and a reaction network for *n*-butyraldehyde self-condensation catalyzed by Ce- $\text{Al}_2\text{O}_3$  was proposed. Subsequently, the research on the intrinsic kinetic of *n*-butyraldehyde self-condensation catalyzed by Ce- $\text{Al}_2\text{O}_3$  showed that both the forward and backward reactions are second order and the corresponding activation energy is separately 79.60 kJ/mol and 74.30 kJ/mol, which is higher than that of the reaction catalyzed by an aqueous base or acid.

### Introduction

As an important chemical, 2-ethylhexanol is mainly used for the production of diethylhexyl phthalate (generally known as dioctyl phthalate, DOP) which serves as a plasticizer for PVC. In addition, 2-ethylhexanol is also used to produce adhesives, surfactants, antioxidants, cosmetics as well as additives of diesel and lubricating oil<sup>1</sup>. The industrial manufacture of 2-ethylhexanol mainly relies on carbonyl synthesis technology and aldehyde condensation technology. Whichever technology is adopted, self-condensation of *n*-butyraldehyde is an essential step. At present, an aqueous caustic alkali catalyst is used for the self-condensation of *n*-butyraldehyde in industry and some drawbacks exist inherently. When the liquid alkali concentration is lower, the condensation reaction proceeds insufficiently and the conversion of *n*-butyraldehyde is lower. When the liquid alkali concentration is much higher, the condensation reaction will take place drastically and the formation of byproducts may lead to a low selectivity of 2-ethyl-2-hexenal. Besides, liquid alkali can corrode reaction apparatus and a lot of liquid acid will be required for handling the spent liquid alkali catalyst. In order to solve the problems resulted from the liquid alkali catalyst, solid base catalysts have drawn much attention for their high activity and

ease of separation. The reported solid base catalysts used for the self-condensation of *n*-butyraldehyde include inorganic<sup>2-4</sup> and organic<sup>5-6</sup> solid bases. However, the solid base catalysts show poor hydrothermal stability and reusability in spite of their high activity, hindering their industrial applications.

The self-condensation of *n*-butyraldehyde is a typical aldol condensation reaction. Aldol condensation reaction can be catalyzed by a basic or an acidic catalyst from the viewpoint of reaction mechanism. The literatures about the self-condensation of *n*-butyraldehyde catalyzed by a solid acid are very few,<sup>7-9</sup> but there are a lot of reports about solid acid-catalyzed other aldol condensation reactions<sup>10-13</sup>. Swift et al.<sup>7</sup> prepared some kinds of supported  $\text{SnO}_2$  catalysts to catalyze the self-condensation of *n*-butyraldehyde and found that acid-base property of a support had a great effect on the catalytic activity: the activity of  $\text{SnO}_2$  supported on an acidic or a basic support was very low while that of neutral silica-supported  $\text{SnO}_2$  was much higher. Under the suitable reaction conditions, the conversion of *n*-butyraldehyde and the selectivity of 2-ethyl-2-hexenal could separately reach 75% and 98% over  $\text{SnO}_2/\text{SiO}_2$  catalyst. Musko et al.<sup>8</sup> studied the catalytic performance of  $\text{H}_4\text{SiW}_{12}\text{O}_{40}/\text{MCM-41}$  in the self-condensation of *n*-butyraldehyde in supercritical carbon dioxide and obtained a 27% of *n*-butyraldehyde conversion and 100% of 2-ethyl-2-hexenal selectivity under the suitable conditions. Compared with the work of Musko et al.<sup>8</sup>, Chen et al.<sup>9</sup> in our group selected  $\text{H}_4\text{SiW}_{12}\text{O}_{40}/\text{SiO}_2$  to catalyze the self-condensation of *n*-butyraldehyde and obtained a better result. Under the suitable conditions, the conversion of *n*-

C. Xiong, N. Liang, H. An, Y. Wang, Prof. Dr. X. Zhao  
School of Chemical Engineering and Technology  
Hebei University of Technology  
GuangRong Dao 8, Hongqiao District  
Tianjin 300130, P. R. China.  
\*Corresponding author e-mail address: zhaoxq@hebut.edu.cn.

butyraldehyde and selectivity of 2-ethyl-2-hexenal could attain 90.4% and 89.2%, respectively. However, the reusability of  $\text{H}_4\text{SiW}_{12}\text{O}_{40}/\text{SiO}_2$  was poor due to the loss of silicotungstic acid. Kikhtyanin et al.<sup>10</sup> evaluated the catalytic performance of a series of molecular sieve catalysts for the aldol condensation of furfural with acetone and found that HBEA(25) showed the best catalytic performance. Under the suitable conditions, the conversion of furfural and the yield of 4-(2-furyl)-3-buten-2-one could reach 50% and 36%, respectively. Lahyani et al.<sup>11</sup> selected acidic resins Amberlyst-15 and Amberlite-200C to catalyze the cross aldol condensation of benzaldehyde with acetophenone. The conversion of benzaldehyde and the yield of chalcone could separately reach 100% and 98% at a reaction temperature = 100 °C and a reaction time = 1 h. However, the yield of chalcone dropped to 72.4% over Amberlyst-15 catalyst and to 77.5% over Amberlyst-200C catalyst after reused for four times. It was evident that the reusability of the two acidic resins was poor. Li et al.<sup>12</sup> prepared Zr-Fe-Cs/SBA-15 by a wetness impregnation to catalyze the aldol condensation of formaldehyde with methyl propionate on a fixed bed reactor and got a 26% of formaldehyde conversion and a 96% of methyl methacrylate selectivity under the suitable conditions. Rekoske et al.<sup>13</sup> utilized anatase  $\text{TiO}_2$  to catalyze the self-condensation of acetaldehyde and obtained a 26% of conversion and a 96% of crotonaldehyde selectivity at a reaction pressure = 0.202 MPa, a reaction temperature = 150 °C and a contact time = 1 min. However, the  $\text{TiO}_2$  catalyst exhibited a rapid deactivation within the first 10 min. In conclusion, HBEA(25), anatase  $\text{TiO}_2$  and Zr-Fe-Cs/SBA-15 showed poor catalytic activity while Amberlyst-15 and Amberlite-200C exhibited a poor reusability. So a catalyst with both high activity and good reusability is expected for aldol condensation reaction.

In this work, we prepared a Ce-modified  $\gamma\text{-Al}_2\text{O}_3$  catalyst which showed good catalytic activity and excellent reusability for the self-condensation of *n*-butyraldehyde. Based on the analysis of the reaction system, a reaction network was proposed and the intrinsic kinetics equation was established.

## Experimental Section

### Preparation of catalysts

$\gamma\text{-Al}_2\text{O}_3$  catalyst was prepared by calcinating pseudo-boehmite on a muffle furnace under air atmosphere. The temperature was controlled as follows: increased from room temperature to 500 °C at a heating-rate of 10 °C/min and then kept for 4 h.

Modified  $\gamma\text{-Al}_2\text{O}_3$  catalysts were prepared by an incipient impregnation of  $\gamma\text{-Al}_2\text{O}_3$  with an aqueous solution of modifier precursor including potassium nitrate, magnesium nitrate, barium nitrate, zinc nitrate, ammonium fluoride, cerium nitrate and boracic acid. The loading of the modifier (in a state of oxide except for fluorine) is 5% (wt). Taking Ce- $\text{Al}_2\text{O}_3$  as an example, the preparation procedure is described as follows. 8 g  $\gamma\text{-Al}_2\text{O}_3$  was impregnated with 9.6 mL of 0.24 M aqueous solution of  $\text{Ce}(\text{NO}_3)_3$  first and then aged at room temperature for 24 h, dried at 110 °C for 8 h and calcinated at 550 °C for 4 h. The preparation of  $\gamma\text{-Al}_2\text{O}_3$  modified by other substances was similar to Ce- $\text{Al}_2\text{O}_3$ .

### Materials Characterization

The textural properties of the catalysts were measured using an ASAP 2020 specific surface area and porosity analyzer made in Micromeritics Company in America. Prior to the test, 0.2 g of the sample was degassed at 150 °C for 4 h in vacuum to remove the impurities adsorbed on the sample surface. Then  $\text{N}_2$  adsorption-desorption test was performed at -195.8 °C. The specific surface area was calculated by the Brunauer-Emmer-Teller (BET) method while the pore volume and pore diameter were calculated by the Barrett-Joyner-Halenda (BJH) method.

The basicity and acidity of a catalyst were measured by a temperature programmed desorption using  $\text{CO}_2$  or  $\text{NH}_3$  as a probe molecule ( $\text{CO}_2\text{-TPD}$ ,  $\text{NH}_3\text{-TPD}$ ) performed on an Auto Chem II 2920 chemical adsorption instrument made in Micromeritics Company in America. Taking the test of  $\text{CO}_2\text{-TPD}$  as example, a typical procedure is described as follows. 0.1 g of the sample was placed in a quartz sample tube under nitrogen atmosphere with a flow of 25 mL/min and then the temperature was increased as follows in order to remove the impurities adsorbed on the sample surface: increased from room temperature to 500 °C at a heating-rate of 10 °C/min and then kept for 1 h. Next the temperature was decreased to 110 °C. Subsequently the sample was saturated with  $\text{CO}_2$  with a flow of 25 mL/min for 30 min. Then the sample was purged by helium with a flow of 50 mL/min for about 1 h to remove the  $\text{CO}_2$  absorbed physically. After that, the temperature was increased to 700 °C at a heating-rate of 10 °C/min. The test of  $\text{NH}_3\text{-TPD}$  is similar to  $\text{CO}_2\text{-TPD}$ .

The X-ray diffraction (XRD) analysis was performed on a Rigaku D/max-2500 X-ray diffractometer using  $\text{Cu K}\alpha$  radiation and a graphite monochromator at 40 kV and 100 mA. The scan range covered from 10° to 90° at a rate of 4 °/min.

X-ray photoelectron spectroscopy (XPS) spectra were recorded with a Physical Electronics Kratos Axis Ultra DLD using monochromatic Al  $\text{K}\alpha$ -rays (1486.6 eV) operated at 150 W and 15 kV. All the spectra with a scan range of 0-1200 eV were obtained with a pass energy of 80 eV and step increment of 1 eV while the narrow-spectra were obtained with a pass energy of 40 eV and 100 mV. The binding energy of C1s (284.6 eV) was used as calibration standard. The obtained XPS peaks were fitted with Peak 4.1 software.

### *n*-Butyraldehyde self-condensation reaction

The self-condensation of *n*-butyraldehyde was conducted in a 100 mL stainless steel autoclave. A typical procedure is described as follows: 40 mL (about 30 g) *n*-butyraldehyde and 4.5 g catalyst were added into the autoclave and then the air inside was replaced with nitrogen. The reaction was conducted at 180 °C for 8 h with a stirring agitation of 400 rpm. After the completion of reaction, the mixture was cooled to room temperature. The catalyst was separated by vacuum filter and the liquid was quantitatively analyzed by a gas chromatograph.

### Product analysis

A qualitative analysis of the reaction products was conducted on a GC-MS (ThermoFinnigan TRACE DSQ). EI ionization source was used in the mass spectrometry with anion source temperature of

200 °C. The mass spectrum was recorded in the range of 40–500 amu. The temperature of both the vaporizing chamber and the transmission line was controlled at 250 °C. A BPX5 capillary column was used for separation of the components and the column temperature was controlled according to the following program: an initial temperature of 40 °C and then heated to 250 °C in a ramp of 10 °C/min and held for 5 min.

A quantitative analysis of the reaction products was carried out using a SP-2100 gas chromatograph (Beijing Beifen-Ruili Analytical Instrument (Group) Co., Ltd). The product mixture was separated in a KB-1 capillary column whose temperature was controlled according to the following program: an initial temperature of 80 °C and held for 3 min, heated to 160 °C in a ramp of 10 °C/min and held for 10 min. Nitrogen was used as a carrier gas and its flow rate was 30 mL/min. The components were analyzed in a flame ionization detector (FID).

## Results and discussion

### 1. Screening of catalysts

The catalytic performance of some solid acids such as  $\gamma$ -Al<sub>2</sub>O<sub>3</sub>, H $\beta$ , HY and HZSM-5 with different molar ratios of Si/Al for the self-condensation of *n*-butyraldehyde was separately investigated and the results are listed in Table 1. It can be seen that the conversion of *n*-butyraldehyde decreased in the following order:  $\gamma$ -Al<sub>2</sub>O<sub>3</sub> > H $\beta$  > HZSM-5(360) > HZSM-5(150) > HZSM-5(38) > HY > HZSM-5(25) > None, and the selectivity of 2-ethyl-2-hexenal lessened as follows:  $\gamma$ -Al<sub>2</sub>O<sub>3</sub> > H $\beta$  > HY > HZSM-5(360) > HZSM-5(150) > None > HZSM-5(38) > HZSM-5(25). It is obvious that  $\gamma$ -Al<sub>2</sub>O<sub>3</sub> showed the best catalytic performance; the conversion of *n*-butyraldehyde and the selectivity of 2-ethyl-2-hexenal reached 83.5% and 84.9%, respectively. Among the three kinds of molecular sieves, HZSM-5 showed the worst catalytic activity. With the increase of the molar ratio of Si/Al, the catalytic activity of HZSM-5 increased gradually, suggesting that strong acidity is unfavorable to the self-condensation of *n*-butyraldehyde. Shen et al.<sup>3</sup> studied the vapor phase self-condensation of *n*-butyraldehyde and found that an ideal catalyst should be neither a strong acid nor a strong base. Furthermore, the catalytic performance of H $\beta$  was higher than HY, in accordance with the result of Komatsu et al.<sup>14</sup> A lower activity of HY may be due to its micropore which hindered the diffusion of the reaction substances.

The acidity of  $\gamma$ -Al<sub>2</sub>O<sub>3</sub>, H $\beta$ , HY and HZSM-5(25) was separately measured and the profiles of NH<sub>3</sub>-TPD and the measurement data are separately shown in Fig.S1 and Table 2. It can be seen that the acid amount of the four solid acids decreased in the following order: HY > HZSM-5 > H $\beta$  >  $\gamma$ -Al<sub>2</sub>O<sub>3</sub> while the acid strength declined as follows: HZSM-5 > HY > H $\beta$  >  $\gamma$ -Al<sub>2</sub>O<sub>3</sub>. The sequence of the acid amount and the acid strength of the three molecular sieves was in consistence with the result determined by Castano et al.<sup>15</sup> Combined with the catalytic performance, it was inferred that the stronger the acidity, the lower the yield of 2-ethyl-2-hexenal. A stronger acidity will give rise to the trimerization of *n*-butyraldehyde, reducing the selectivity of 2-ethyl-2-hexenal. A weaker acidity of  $\gamma$ -Al<sub>2</sub>O<sub>3</sub> is responsible for its better catalytic performance. Besides, with the increase of the molar ratio of Si/Al,

the acid strength of HZSM-5 decreased, and the selectivity and the yield of 2-ethyl-2-hexenal increased because of restraining the occurrence of side-reactions. Therefore, the weak acid sites could contribute to the self-condensation of *n*-butyraldehyde. Ungureanu et al.<sup>16</sup> obtained a similar conclusion using UL-ZSM-5 to catalyze the aldol condensation of formaldehyde with acetaldehyde. Thereby,  $\gamma$ -Al<sub>2</sub>O<sub>3</sub> was chosen as the catalyst to do a further research in this work.

**Table 1** Catalytic performance of different solid acid catalysts

Catalyst	X <sub>BA</sub> /%	Y <sub>2E2H</sub> /%	S <sub>2E2H</sub> /%
None	41.3	12.6	30.5
$\gamma$ -Al <sub>2</sub> O <sub>3</sub>	83.5	70.8	84.9
H $\beta$	77.3	51.6	66.8
HY	52.9	29.2	55.3
HZSM-5 (360)	62.6	28.1	45.0
HZSM-5 (150)	57.8	21.9	37.8
HZSM-5(38)	53.3	14.9	28.0
HZSM-5(25)	49.3	9.6	19.6

Reaction conditions: a weight percentage of catalyst = 10%, T = 180 °C, t = 6 h.

BA: *n*-butyraldehyde; 2E2H: 2-ethyl-2-hexenal; X: conversion; Y: yield; S: selectivity.

### 2. Preparation and catalytic performance of $\gamma$ -Al<sub>2</sub>O<sub>3</sub>

$\gamma$ -Al<sub>2</sub>O<sub>3</sub> catalyst was prepared by calcinating pseudo-boehmite as described in Experimental Section. The effect of calcination temperature and calcination time on the textural structure and catalytic performance  $\gamma$ -Al<sub>2</sub>O<sub>3</sub> was investigated and the details are enclosed in the Supporting Information. As a result, the suitable preparation conditions of  $\gamma$ -Al<sub>2</sub>O<sub>3</sub> were as follows: pseudo-boehmite was calcinated at 500 °C for 4 h. The catalytic performance of  $\gamma$ -Al<sub>2</sub>O<sub>3</sub> prepared at above conditions was evaluated at different reaction conditions. The effect of reaction parameters on the catalytic performance is enclosed in the Supporting Information. The results showed that  $\gamma$ -Al<sub>2</sub>O<sub>3</sub> dosage, reaction temperature, and reaction time exerted different influence on the catalytic performance of  $\gamma$ -Al<sub>2</sub>O<sub>3</sub>. The suitable reaction conditions for *n*-butyraldehyde self-condensation over  $\gamma$ -Al<sub>2</sub>O<sub>3</sub> catalyst were obtained as follows: a weight percentage of  $\gamma$ -Al<sub>2</sub>O<sub>3</sub> catalyst = 15%, a reaction temperature = 180 °C, and a reaction time = 8 h. The yield of 2-ethyl-2-hexenal was 76.6% at a *n*-butyraldehyde conversion of 87% under the above reaction conditions.

### 3. Modification of $\gamma$ -Al<sub>2</sub>O<sub>3</sub>

As mentioned above, the yield of 2-ethyl-2-hexenal was merely 76.6% under the suitable reaction conditions, lower than the data obtained from the industrial aqueous caustic alkali, indicating that the catalytic performance of  $\gamma$ -Al<sub>2</sub>O<sub>3</sub> was not satisfactory. Thereby, a modification of  $\gamma$ -Al<sub>2</sub>O<sub>3</sub> is needed in order to improve its catalytic performance.

#### 3.1 Screening of modifier

Aldol condensation reaction can be catalyzed by either acid or base, so the acidity and basicity of a catalyst will have a great impact on its catalytic performance.  $\gamma$ -Al<sub>2</sub>O<sub>3</sub> is traditionally

## Journal Name

## ARTICLE

considered as a weak solid acid but there are both acid sites and base sites on its surface. Therefore, it is expected to enhance its catalytic performance by introducing a kind of modifier to tune its superficial acidity and basicity. A promotion in the basicity of  $\gamma$ -Al<sub>2</sub>O<sub>3</sub> was expected by the introduction of potassium oxide,

magnesium oxide, and barium oxide while introducing boric oxide and fluorine could increase the acidity of  $\gamma$ -Al<sub>2</sub>O<sub>3</sub>. A fine tuning of the acidity and basicity of  $\gamma$ -Al<sub>2</sub>O<sub>3</sub> might be achieved by introducing zinc oxide and cerium oxide.

**Table 2** Acidic properties of some solid acid catalysts

Catalyst	NH <sub>3</sub> desorption peak at lower temperature		NH <sub>3</sub> desorption peak at higher temperature		Total acid amount / $\mu\text{mol g}^{-1}$
	Peak top temperature / $^{\circ}\text{C}$	Weak acid amount / $\mu\text{mol g}^{-1}$	Peak top temperature / $^{\circ}\text{C}$	Strong acid amount / $\mu\text{mol g}^{-1}$	
$\gamma$ -Al <sub>2</sub> O <sub>3</sub>	176.1	386.6	/	/	386.6
H $\beta$	179.2	359.4	273.4	348.1	707.8
HY	192.0	838.8	334.1	1226.5	2065.3
HZSM-5(25)	195.5	680.7	398.2	757.6	1438.3

**Table 3** Catalytic performance of the modified  $\gamma$ -Al<sub>2</sub>O<sub>3</sub> catalysts

Catalyst	X <sub>BA</sub> /%	Y <sub>2E2H</sub> /%	S <sub>2E2H</sub> /%
$\gamma$ -Al <sub>2</sub> O <sub>3</sub>	87.5	76.6	87.5
B-Al <sub>2</sub> O <sub>3</sub>	81.3	67.1	82.5
F-Al <sub>2</sub> O <sub>3</sub>	88.0	73.9	83.9
Zn-Al <sub>2</sub> O <sub>3</sub>	86.3	75.6	87.6
Ba-Al <sub>2</sub> O <sub>3</sub>	84.9	74.4	87.5
Mg-Al <sub>2</sub> O <sub>3</sub>	86.7	78.1	90.0
K-Al <sub>2</sub> O <sub>3</sub>	87.6	78.7	89.8
Ce-Al <sub>2</sub> O <sub>3</sub>	93.8	83.1	88.6

Reaction conditions: a weight percentage of catalyst =15%, T=180 $^{\circ}\text{C}$ , t=8 h.

BA: *n*-butyraldehyde; 2E2H: 2-ethyl-2-hexenal; X: conversion; Y: yield; S: selectivity

**Table 4** Acid and base properties of different modified  $\gamma$ -Al<sub>2</sub>O<sub>3</sub> catalysts

Catalyst	Acid property		Base property				
	NH <sub>3</sub> desorption peak / $^{\circ}\text{C}$	Total acid amount / $\mu\text{mol g}^{-1}$	CO <sub>2</sub> desorption peak at lower temperature		CO <sub>2</sub> desorption peak at higher temperature		Total base amount / $\mu\text{mol g}^{-1}$
			Peak top temperature / $^{\circ}\text{C}$	Weak base amount / $\mu\text{mol g}^{-1}$	Peak top temperature / $^{\circ}\text{C}$	Strong base amount / $\mu\text{mol g}^{-1}$	
$\gamma$ -Al <sub>2</sub> O <sub>3</sub>	176.1	386.6	163.3	29.1	378.0	179.1	178.2
B-Al <sub>2</sub> O <sub>3</sub>	181.6	500.4	—	—	331.1	113.7	113.7
F-Al <sub>2</sub> O <sub>3</sub>	181.0	306.6	—	—	317.7	116.1	116.1
Zn-Al <sub>2</sub> O <sub>3</sub>	191.4	463.0	167.6	19.3	336.6	162.7	182.0
Ba-Al <sub>2</sub> O <sub>3</sub>	186.8	254.8	172.3	18.7	281.9	142.8	161.5
Mg-Al <sub>2</sub> O <sub>3</sub>	189.3	484.0	171.6	756.1	—	—	756.1
K-Al <sub>2</sub> O <sub>3</sub>	187.0	100.8	167.3	641.3	—	—	641.3
Ce-Al <sub>2</sub> O <sub>3</sub>	191.9	404.8	172.7	540.3	—	—	540.3

The catalytic performances of  $\gamma$ -Al<sub>2</sub>O<sub>3</sub> modified by different substances are listed in Table 3. The loading of the modifier (based on oxide except for F) accounted for 5% (wt) of  $\gamma$ -Al<sub>2</sub>O<sub>3</sub>. It was obvious that modifier had an important influence on the catalytic performance of  $\gamma$ -Al<sub>2</sub>O<sub>3</sub>. The catalytic performance of  $\gamma$ -Al<sub>2</sub>O<sub>3</sub> modified by nonmetal B and F was the worst; the selectivity of 2-ethyl-2-hexenal decreased. Especially for B-Al<sub>2</sub>O<sub>3</sub>, the selectivity and yield of 2-ethyl-2-hexenal were merely 82.5% and 67.1%. In contrast, the  $\gamma$ -Al<sub>2</sub>O<sub>3</sub> modified by metallic oxide showed good catalytic performance. The selectivity of 2-ethyl-2-hexenal reached the highest, 90.0%, over Mg-Al<sub>2</sub>O<sub>3</sub> catalyst. Moreover, Ce-Al<sub>2</sub>O<sub>3</sub> exhibited the best catalytic performance and the yield of 2-ethyl-2-hexenal was the highest, up to 83.1%. So Ce was determined to be the suitable modifier.

Acid and base properties of the modified  $\gamma$ -Al<sub>2</sub>O<sub>3</sub> catalysts were measured and the profiles of NH<sub>3</sub>-TPD and CO<sub>2</sub>-TPD are separately shown in Fig.S6, Fig.S7, Fig.S8, Fig.S9, Fig.S10 and Fig.S11 while the measurement data are summarized in Table 4. After modified by nonmetal B and F, the total base amount of  $\gamma$ -Al<sub>2</sub>O<sub>3</sub> dropped distinctly and the base strength also decreased and the weak base sites of  $\gamma$ -Al<sub>2</sub>O<sub>3</sub> disappeared. The total acid amount rose for the  $\gamma$ -Al<sub>2</sub>O<sub>3</sub> modified by B but decreased for the  $\gamma$ -Al<sub>2</sub>O<sub>3</sub> modified by F. Furthermore, a new strong acid site appeared and the acid strength was enhanced after modified by F. Jian et al.<sup>17</sup> studied the role of F in the  $\gamma$ -Al<sub>2</sub>O<sub>3</sub> catalyst and obtained a similar conclusion. They considered that the lone pair electrons of F was in coordination with the acid sites on the surface of  $\gamma$ -Al<sub>2</sub>O<sub>3</sub> and the acid sites of  $\gamma$ -Al<sub>2</sub>O<sub>3</sub> were covered partly, causing the reduction of the acid amount. Meanwhile, the higher electro-negativity of F had a great inductive effect and could make the strength of acid site nearby stronger. When modified by transition metal Zn, the total acid amount of  $\gamma$ -Al<sub>2</sub>O<sub>3</sub> rose but the total base amount and base strength changed a little. Through the modification of alkaline earth metal Ba, the total acid amount of  $\gamma$ -Al<sub>2</sub>O<sub>3</sub> dropped severely but the total base amount declined slightly. After modified by alkali metal K, alkaline earth Mg and rare-earth metal Ce, all the desorption peaks of CO<sub>2</sub> at higher temperature disappeared but the total base amount increased drastically. In addition, the total acid amount of  $\gamma$ -Al<sub>2</sub>O<sub>3</sub> modified by Mg and Ce increased to some extent but decreased when modified by K. Shen et al.<sup>3</sup> found that the silica-supported MgO and SrO catalysts had a dramatically increased NH<sub>3</sub> uptake because of the formation of extra acid sites. It was also observed in Table 4 that the influence of different substances on the base amount of  $\gamma$ -Al<sub>2</sub>O<sub>3</sub> was much greater than that on its acid amount. The base amount declined in the following order: Mg-Al<sub>2</sub>O<sub>3</sub> > K-Al<sub>2</sub>O<sub>3</sub> > Ce-Al<sub>2</sub>O<sub>3</sub> > Zn-Al<sub>2</sub>O<sub>3</sub> >  $\gamma$ -Al<sub>2</sub>O<sub>3</sub> > Ba-Al<sub>2</sub>O<sub>3</sub> > F-Al<sub>2</sub>O<sub>3</sub> ≈ B-Al<sub>2</sub>O<sub>3</sub>. Combined with the catalytic performance, we can see that the base amount played a major role in the improvement of the selectivity of 2-ethyl-2-hexenal. With respect to B-Al<sub>2</sub>O<sub>3</sub> and F-Al<sub>2</sub>O<sub>3</sub> with lower base

amount, the selectivity of 2-ethyl-2-hexenal was higher over Mg-Al<sub>2</sub>O<sub>3</sub>, K-Al<sub>2</sub>O<sub>3</sub> and Ce-Al<sub>2</sub>O<sub>3</sub> catalysts with higher base amount. As a consequence, it was inferred that the base amount of the modified  $\gamma$ -Al<sub>2</sub>O<sub>3</sub> is the key factor influencing the selectivity of 2-ethyl-2-hexenal; the bigger the base amount, the higher the selectivity of 2-ethyl-2-hexenal. Climent et al.<sup>18</sup> compared the selectivity of MgO and NaCsX zeolite in the aldol condensation of heptanal with benzaldehyde and found that base strength certainly had an important influence on the selectivity. In this study, it is found that weak base amount played a crucial role in the selectivity. Not only does Ce-Al<sub>2</sub>O<sub>3</sub> have relatively higher base amount, but also its 4f electronic structure is beneficial to the polarization of a carbonyl group,<sup>19</sup> promoting the formation of enol structure which is good for the enhancement of the conversion of *n*-butyraldehyde. In addition, the excellent catalytic performance of Ce-Al<sub>2</sub>O<sub>3</sub> is possibly attributed to its suitable and matched acid-base properties on the surface.

### 3.2 Effect of Ce loading

The catalytic performance of Ce-Al<sub>2</sub>O<sub>3</sub> with different loading amounts of Ce was evaluated and the results are shown in Fig. 1. With the increase of the loading amount of Ce, the conversion of *n*-butyraldehyde increased at first and then decreased, similar to the selectivity of 2-ethyl-2-hexenal. The conversion of *n*-butyraldehyde reached the maximum over the Ce-Al<sub>2</sub>O<sub>3</sub> with the Ce loading amount of 5% while the selectivity of 2-ethyl-2-hexenal attained the maximum over the Ce-Al<sub>2</sub>O<sub>3</sub> with the Ce loading amount of 7%. Since the yield of 2-ethyl-2-hexenal achieved the maximum over the Ce-Al<sub>2</sub>O<sub>3</sub> with the Ce loading amount of 5%, 5% was chosen as the suitable loading amount of Ce. In order to elucidate the role of Ce in Ce-Al<sub>2</sub>O<sub>3</sub>, CeO<sub>2</sub> was used to catalyze the self-condensation of *n*-butyraldehyde under the suitable reaction conditions. The conversion of *n*-butyraldehyde and the yield of 2-ethyl-2-hexenal attained 71.3% and 29.9%, respectively, far lower than the catalytic performance of  $\gamma$ -Al<sub>2</sub>O<sub>3</sub>. It is obvious that CeO<sub>2</sub> played a role of a promoter not a major active species.

### 3.3 Analysis of Ce function

Fig.S12 presents deconvoluted XPS spectra of Ce3d of the fresh Ce-Al<sub>2</sub>O<sub>3</sub>. The spin-orbit peaks of 'a' and 'e' centered at 898.3 eV and 916.4 eV are attributed to the primary photoionization from Ce<sup>4+</sup> with Ce3d<sup>9</sup>4f<sup>0</sup>O2p<sup>6</sup> final state<sup>20</sup>. The spin-orbit peaks of f-b, i-d and g-h with lower binding energy are assigned to the Ce3d<sup>9</sup>4f<sup>1</sup>O2p<sup>5</sup> and Ce3d<sup>9</sup>4f<sup>2</sup>O2p<sup>4</sup> final states shake-down satellite features<sup>20</sup>. Those satellite peaks are caused by the charge transfer from ligand (O2p) to metal (Ce4f) in the primary photoionization process. The peaks of 'c' and 'i' centered at 885.5 eV and 903.9 eV are associated with Ce<sup>3+</sup> final states. In this sense, c-i spin-orbit doublet peaks are assigned to the main photoionization from Ce3d<sup>9</sup>4f<sup>1</sup>O2p<sup>6</sup> final state<sup>20</sup>. Fig.S13 shows the XPS spectra of Ce3d of the recovered Ce-

Al<sub>2</sub>O<sub>3</sub> without calcination. Compared with Fig.S12, it is not difficult to find that the peak of 'a' at 916.4 eV completely disappears in Fig.S13, probably due to the lack of 4f<sup>0</sup> configuration in the formation of Ce<sup>3+</sup> state. Thus, any transitions involving the 4f<sup>0</sup> configuration will not appear in the spectra<sup>21</sup>. Meanwhile, the area of peak 'e' at 898.3 eV decreases drastically while that of peaks at the 903.9 eV and 885.4 eV corresponding to Ce<sup>3+</sup> species increases greatly. Cerium oxide is known to possess a very high oxygen exchange capacity which is related to the ability of reversible change of oxidation states of cerium between Ce<sup>4+</sup> and Ce<sup>3+</sup>. Additionally, the reduction of Ce species is not resulted from a direct release of O<sub>2</sub> to the gas phase but from a surface reaction with a reductant such as CO or a hydrocarbon<sup>22</sup>. Therefore, it is speculated that some kind of reductants existing in the reaction system of *n*-butyraldehyde self-condensation reduced Ce species from Ce<sup>4+</sup> to Ce<sup>3+</sup>. Shyu et al.<sup>21</sup> obtained a similar conclusion that CeAlO<sub>3</sub> was formed from CeO<sub>2</sub>-Al<sub>2</sub>O<sub>3</sub> in H<sub>2</sub> or under vacuum at elevated temperatures. Fig.S14 shows the XPS spectra of Ce3d of the recovered Ce-Al<sub>2</sub>O<sub>3</sub> calcinated at 550 °C for 4 h. Compared with Fig.S13, it can be observed that the peak area of Ce<sup>3+</sup> species at 903.9 eV and 885.4 eV decreases to a small degree while other peaks change little. New peaks of 'A' and 'C' appear which belong to the Ce<sup>4+</sup> species. It is obvious that Ce<sup>3+</sup> species could be transformed to Ce<sup>4+</sup> species after the recovered Ce-Al<sub>2</sub>O<sub>3</sub> was calcinated. He et al.<sup>23</sup> thought that trivalent cerium species could convert into tetravalent cerium species in the presence of the oxidants such as oxygen under alkaline conditions. Shyu et al.<sup>21</sup> gained a similar conclusion that CeAlO<sub>3</sub> precursor could be reoxidized to CeO<sub>2</sub> even at room temperature upon exposure to oxidizing environments.

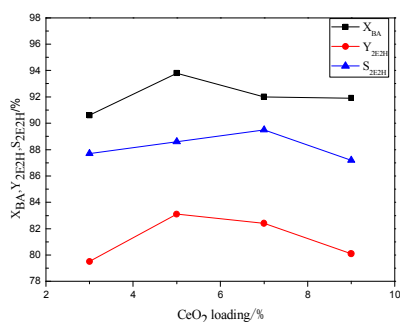


Fig. 1 Effect of CeO<sub>2</sub> loading on the catalytic performance of  $\gamma$ -Al<sub>2</sub>O<sub>3</sub> catalyst

Reaction conditions: a weight percentage of catalyst = 15%, T = 180 °C, t = 8 h.

X: conversion; Y: yield; S: selectivity;

BA: *n*-butyraldehyde; 2E2H: 2-ethyl-2-hexenal.

The peak areas (A) of Ce<sup>4+</sup> and Ce<sup>3+</sup> species are used to estimate their relative contents (C) in the Ce-Al<sub>2</sub>O<sub>3</sub> using the following equations and the results in the fresh Ce-Al<sub>2</sub>O<sub>3</sub>, the recovered Ce-Al<sub>2</sub>O<sub>3</sub> without calcination and the recovered Ce-Al<sub>2</sub>O<sub>3</sub> after calcination are separately listed in Table 5, Table 6 and Table 7.

$$C_{Ce^{4+}} = \frac{\sum A_{Ce^{4+}}}{\sum A_{Ce^{4+}} + \sum A_{Ce^{3+}}}$$

It is known from the calculation result that the percentage of Ce<sup>4+</sup> species was 94% in the fresh Ce-Al<sub>2</sub>O<sub>3</sub>, and dropped to 10% in the recovered Ce-Al<sub>2</sub>O<sub>3</sub> without calcination and increased back to 42% in the recovered Ce-Al<sub>2</sub>O<sub>3</sub> after calcination. It can be seen from Table 8 that the conversion of *n*-butyraldehyde decreased to some extent while the selectivity of 2-ethyl-2-hexenal decreased greatly for the recovered Ce-Al<sub>2</sub>O<sub>3</sub> without calcination as compared with the fresh Ce-Al<sub>2</sub>O<sub>3</sub>. Thus, it is certain that the Ce<sup>4+</sup> species are the active sites in Ce-Al<sub>2</sub>O<sub>3</sub>. On the other hand, the percentage of Ce<sup>4+</sup> species in the recovered Ce-Al<sub>2</sub>O<sub>3</sub> after calcination is less than half of that in the fresh Ce-Al<sub>2</sub>O<sub>3</sub> but the catalytic activity of the recovered Ce-Al<sub>2</sub>O<sub>3</sub> after calcination is almost the same as the fresh one. Therefore, it is inferred that the valence state of Ce affects the catalytic performance of Ce-Al<sub>2</sub>O<sub>3</sub> to some extent but it does not play a key role in the catalytic performance. As mentioned above, the acid and base property of  $\gamma$ -Al<sub>2</sub>O<sub>3</sub> catalyst exerts a great effect on the catalytic performance and furthermore the base amount is the key factor influencing the selectivity of 2-ethyl-2-hexenal. Therefore, it is speculated that the acid and base property of Ce-Al<sub>2</sub>O<sub>3</sub> play a dominant role in its catalytic performance.

Acid and base properties of the fresh and the recovered Ce-Al<sub>2</sub>O<sub>3</sub> catalysts were measured and the profiles of CO<sub>2</sub>-TPD and NH<sub>3</sub>-TPD are separately shown in Fig.S15 and Fig.S16 while the measurement data are summarized in Table S2. As compared with the fresh Ce-Al<sub>2</sub>O<sub>3</sub>, the total acid amount decreased to some extent and what is more, a new strong acid site appeared while the total base amount increased greatly but the base strength increased a little in the recovered Ce-Al<sub>2</sub>O<sub>3</sub> without calcination. After calcinated at 550 °C for 4 h, both the base amount and strength decreased and furthermore the base strength restored to that of the fresh Ce-Al<sub>2</sub>O<sub>3</sub>. The new strong acid site disappeared and both the weak acid amount and strength increased and furthermore the weak acid strength restored to that of the fresh Ce-Al<sub>2</sub>O<sub>3</sub>. In a word, the acid and base properties of the recovered Ce-Al<sub>2</sub>O<sub>3</sub> after calcination restored almost to those of the fresh Ce-Al<sub>2</sub>O<sub>3</sub>.

$\gamma$ -Al<sub>2</sub>O<sub>3</sub> can be hydrated with the byproduct water to form boehmite phase in the aldol condensation of *n*-butyraldehyde.<sup>32</sup> Since the acid amount of  $\gamma$ -Al<sub>2</sub>O<sub>3</sub> is more than boehmite<sup>33</sup>, it is speculated that the increase of the base amount and the decrease of the acid amount in the recovered Ce-Al<sub>2</sub>O<sub>3</sub> without calcination is related to the formation of boehmite. Boehmite can decompose to  $\gamma$ -Al<sub>2</sub>O<sub>3</sub> after calcination<sup>34</sup>, so the base amount decreased and acid amount increased in the recovered Ce-Al<sub>2</sub>O<sub>3</sub> after calcination. Combined with the result of Table S2 and Table 8, it is inferred that the strong acid site does harm to the self-condensation of *n*-butyraldehyde, causing the side-reactions to reduce the selectivity of 2-ethyl-2-hexenal. Zeidan et. al<sup>35</sup> selected the acid-base bifunctionalized mesoporous SBA-15 to catalyze the aldol condensation of 4-nitrobenzaldehyde with acetone and found that the catalytic activity of bifunctionalized materials increased gradually with the decrease of the acidity.

It can be seen from Table 8 that the conversion of *n*-butyraldehyde changed little while the selectivity of 2-ethyl-2-hexenal decreased greatly over the recovered Ce-Al<sub>2</sub>O<sub>3</sub> without calcination as compared with the fresh Ce-Al<sub>2</sub>O<sub>3</sub>. Despite the fact that the total base amount increased for the recovered Ce-Al<sub>2</sub>O<sub>3</sub>

without calcination, the appearance of the strong acid site reduced its catalytic activity, so its selectivity of 2-ethyl-2-hexenal decreased. After calcination at 550 °C for 4 h, the total base site amount decreased and was slightly more than that of the fresh Ce-Al<sub>2</sub>O<sub>3</sub> while the strong acid site disappeared, so the catalytic performance was restored for the recovered Ce-Al<sub>2</sub>O<sub>3</sub> after calcination. In conclusion, matchable acid and base properties are the key factor to achieve a good catalytic performance of Ce-Al<sub>2</sub>O<sub>3</sub>.

**Table 5** Binding energies, valence states and relative contents of Ce3d in the fresh Ce-Al<sub>2</sub>O<sub>3</sub>

Peak assignment	Ce species	Binding energy (eV)	C <sub>Ce<sup>3+</sup></sub> (%)	Refs
a	Ce <sup>4+</sup>	916.4	15	23
b	Ce <sup>4+</sup>	906.1	15	20
c	Ce <sup>3+</sup>	903.9	2	24
d	Ce <sup>4+</sup>	901.0	14	25
e	Ce <sup>4+</sup>	898.3	15	26
f	Ce <sup>4+</sup>	889.1	6	27
g	Ce <sup>4+</sup>	887.6	1	28
h	Ce <sup>4+</sup>	886.7	4	29
i	Ce <sup>3+</sup>	885.4	4	22
j	Ce <sup>4+</sup>	882.4	24	30

**Table 6** Binding energies, valence states and relative contents of Ce3d in the recovered Ce-Al<sub>2</sub>O<sub>3</sub> without calcination

Peak assignment	Ce species	Binding energy (eV)	C <sub>Ce<sup>3+</sup></sub> (%)	Refs
1	Ce <sup>3+</sup>	904.1	38	24
2	Ce <sup>4+</sup>	901.7	3	25
3	Ce <sup>4+</sup>	899.0	3	26
4	Ce <sup>3+</sup>	885.5	48	24
5	Ce <sup>4+</sup>	883.1	4	23
6	Ce <sup>3+</sup>	881.3	4	30

**Table 7** Binding energies, valence states and relative contents of Ce3d in the recovered Ce-Al<sub>2</sub>O<sub>3</sub> after calcination

Peak assignment	Ce species	Binding energy (eV)	C <sub>Ce<sup>3+</sup></sub> (%)	Refs
A	Ce <sup>4+</sup>	916.8	7	23
B	Ce <sup>4+</sup>	911.8	2	31
C	Ce <sup>4+</sup>	907.9	5	20
D	Ce <sup>3+</sup>	904.1	29	24
E	Ce <sup>4+</sup>	901.4	5	25
F	Ce <sup>4+</sup>	898.6	10	26
G	Ce <sup>3+</sup>	885.5	28	24
H	Ce <sup>4+</sup>	882.8	13	22
I	Ce <sup>3+</sup>	881.3	1	30

**Table 8** Catalytic performance of different catalysts for the self-condensation of *n*-butyraldehyde

Catalyst	X <sub>BA</sub> /%	Y <sub>2E2H</sub> /%	S <sub>2E2H</sub> /%
Fresh Ce-Al <sub>2</sub> O <sub>3</sub>	93.7	80.3	85.7
Recovered Ce-Al <sub>2</sub> O <sub>3</sub>			
Without calcination	90.3	71.1	78.8
Recovered Ce-Al <sub>2</sub> O <sub>3</sub> after calcination	93.3	83.0	88.9
$\gamma$ -Al <sub>2</sub> O <sub>3</sub>	86.6	72.9	84.2

Reaction conditions: a weight percentage of catalyst = 15%, T = 180 °C, t = 8 h.

BA: *n*-butyraldehyde; 2E2H: 2-ethyl-2-hexenal; X: conversion; Y: yield; S: selectivity.

### 3.4 Reusability of Ce-Al<sub>2</sub>O<sub>3</sub>

The reusability of Ce-Al<sub>2</sub>O<sub>3</sub> after calcination was investigated and the results are listed in Table 9. It can be seen that after reused for several times, the selectivity of 2-ethyl-2-hexenal rose slightly while the conversion of *n*-butyraldehyde declined a little. The increase of the selectivity is in accordance with the increase of the base amount of the recovered Ce-Al<sub>2</sub>O<sub>3</sub> after calcination (see Table S2). On the whole, the catalyst Ce-Al<sub>2</sub>O<sub>3</sub> showed good stability: the yield of 2-ethyl-2-hexenal decreased merely by 0.6% when reused for four times.

**Table 9** Reusability of Ce modified  $\gamma$ -Al<sub>2</sub>O<sub>3</sub>

Run	X <sub>BA</sub> /%	Y <sub>2E2H</sub> /%	S <sub>2E2H</sub> /%
1	93.8	83.1	88.6
2	93.3	83.0	88.9
3	92.4	82.5	89.2
4	91.3	82.5	90.4
5	91.0	82.5	90.7

Reaction conditions: a weight percentage of catalyst = 15%, T = 180 °C, t = 8 h.

BA: *n*-butyraldehyde; 2E2H: 2-ethyl-2-hexenal; X: conversion; Y: yield; S: selectivity.

### 4. Analysis of reaction system

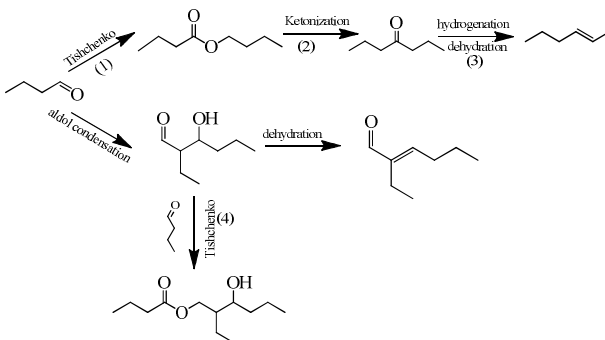
The reaction liquid obtained from the self-condensation of *n*-butyraldehyde catalyzed by Ce-Al<sub>2</sub>O<sub>3</sub> was analyzed by GC-MS and results listed in Table S3 show that several by-products were found such as butyl butyrate, 4-heptanone, 3-heptylene, 2-ethyl-3-hydroxyhexyl butyrate and so on. Based on the analysis results of GC-MS, some side-reactions (1)~(4) were speculated as Scheme 1.

Tsuji et al.<sup>36</sup> thought that Al<sub>2</sub>O<sub>3</sub> can catalyze the Tishchenko reaction of *n*-butyraldehyde to produce butyl butyrate, so the reaction (1) was speculated. Shen et al.<sup>3</sup> probed into the vapor phase self-condensation of *n*-butyraldehyde catalyzed by alkaline earth metal oxide and discovered that the reaction system contained C7 alkene byproduct. At present, there is a dispute on the formation of C7 alkene. Idriss et al.<sup>37</sup> considered that C7 alkene came from the reductive coupling reaction of *n*-butyraldehyde. Luo



et al.<sup>38</sup> believed that the reductive coupling reaction was prone to occurrence on the surface of a reductant and there was a great possibility that C7 alkene was originated from these side-reactions such as dehydroxylation and decarbonylation. Shen et al.<sup>3</sup> deemed that C7 alkene may be derived from the hydrogenation/dehydration of heptanone generated from the ketonization of butyl butyrate. Glinski et al.<sup>39</sup> studied the ketonization of ethyl heptanoate catalyzed by Ce or Zr loaded Al<sub>2</sub>O<sub>3</sub> and found the formation of 13 ketone, ethylene, carbon dioxide and water. On the basis of above discussion, the reaction (2) was inferred. Namely the ketonization of butyl butyrate generated carbon dioxide, water, 1-butene and heptanone followed by a hydrogenation/dehydration to produce C7 alkene. The hydrogen used for the hydrogenation was derived from the decomposition of *n*-butyraldehyde.<sup>37</sup> The formation of 2-ethyl-2-hexenal comprises two reaction steps: the condensation of *n*-butyraldehyde to 2-ethyl-3-hydroxyhexanal and the dehydration of the intermediate to 2-ethyl-2-hexenal. Part of 2-ethyl-3-hydroxyhexanal could react with *n*-butyraldehyde to produce 2-ethyl-3-hydroxyhexyl butyrate by the Tishchenko reaction, described as reaction (4), in accordance with the result obtained by Zhu et al.<sup>40</sup> and Tsuji et al.<sup>36</sup> Zhu et al.<sup>40</sup> used rare earth compound to catalyze aldol condensation-Tishchenko reaction of *n*-butyraldehyde and found that 2-ethyl-3-hydroxyhexyl butyrate was formed. Tsuji et al.<sup>36</sup> concluded that Al<sub>2</sub>O<sub>3</sub> could catalyze the Tishchenko reaction of *n*-butyraldehyde to produce 2-ethyl-3-hydroxyhexyl butyrate and furthermore *n*-butyraldehyde preferred to react with 2-ethyl-3-hydroxyhexanal by the cross-Tishchenko reaction, compared with the self-Tishchenko reaction of *n*-butyraldehyde.

Based on the results of product analysis and discussion above, a possible reaction network for self-condensation of *n*-butyraldehyde catalyzed by Ce-Al<sub>2</sub>O<sub>3</sub> was proposed as shown in Scheme 1. A majority of *n*-butyraldehyde undertakes aldol condensation to 2-ethyl-3-hydroxyhexanal followed by a dehydration reaction to 2-ethyl-2-hexenal. Simultaneously, a minority of *n*-butyraldehyde will be converted to butyl butyrate by the Tishchenko reaction and then butyl butyrate can transform to heptanone from the ketonization followed by a hydrogenation/dehydration to C7 alkene. In addition, a small quantity of 2-ethyl-3-hydroxyhexanal can react with one molecule of *n*-butyraldehyde by the Tishchenko reaction to produce 2-ethyl-3-hydroxyhexyl butyrate.



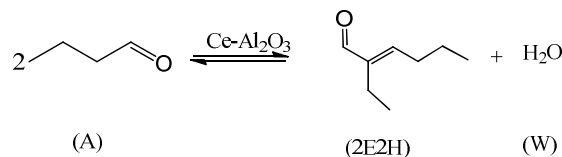
**Scheme 1** Reaction network of *n*-butyraldehyde self-condensation catalyzed by Ce-Al<sub>2</sub>O<sub>3</sub>

## 5. Kinetic study

In order to get an intensive investigation of the *n*-butyraldehyde self-condensation reaction catalyzed by Ce-Al<sub>2</sub>O<sub>3</sub>, its intrinsic reaction kinetics was established. The influence of internal and external diffusion was eliminated prior to the kinetic experiments.

### 5.1 Establishment of kinetic model and estimation of parameters

The *n*-butyraldehyde self-condensation reaction can be described as follows:



The rate of a chemical reaction ( $r_A$ ) is the function of the concentration of reaction components ( $C_A$ ,  $C_{2E2H}$ ,  $C_W$ ) and reaction temperature ( $T$ ).  $C_A$ ,  $C_{2E2H}$  and  $C_W$  can be expressed by means of the conversion of *n*-butyraldehyde ( $x_A$ ). The reaction rate equation can be described as follows:

$$r_A = -\frac{1}{V} \frac{dn_A}{dt} = \frac{n_{A0}}{V} \frac{dx_A}{dt} = k_+ C_A^m - k_- C_{2E2H}^p C_W^q \quad (5)$$

because  $C_{2E2H} = \frac{n_{2E2H}}{V} = \frac{n_{A0} \times x_A}{2V} = C_{A0} \times \frac{x_A}{2} = C_W$ , eq (5) can be converted to eq (6):

$$C_{A0} \frac{dx_A}{dt} = k_+ C_{A0}^m (1-x_A)^m - k_- C_{A0}^{(p+q)} \left(\frac{x_A}{2}\right)^{(p+q)} \quad (6)$$

Suppose  $p+q=n$ , eq (6) can be changed as follows:

$$C_{A0} \frac{dx_A}{dt} = k_+ C_{A0}^m (1-x_A)^m - k_- C_{A0}^n \left(\frac{x_A}{2}\right)^n \quad (7)$$

When the Arrhenius equation  $k = A \exp\left(\frac{-Ea}{RT}\right)$  is put into eq (7), the differential equation to be fitted can be shown as follows:

$$\frac{dx_A}{dt} = A_+ \exp\left(\frac{-Ea_+}{RT}\right) C_{A0}^{m-1} (1-x_A)^m - A_- \exp\left(\frac{-Ea_-}{RT}\right) C_{A0}^{n-1} \left(\frac{x_A}{2}\right)^n \quad (8)$$

Where  $x_A$  is the conversion of *n*-butyraldehyde,  $t$  and  $T$  are separately the reaction time and reaction temperature. The pre-exponential factor  $A_+$  and  $A_-$ , the activation energy  $Ea_+$  and  $Ea_-$  and the reaction order  $m$  and  $n$  are the parameters to be determined. It has been known that  $R = 8.314 \text{ J}/(\text{mol}\cdot\text{K})$  and the initial concentration of *n*-butyraldehyde  $C_{A0} = 11.09 \text{ mol/L}$ . The kinetic experiment was conducted on an autoclave and the time when the temperature inside the autoclave reached the reaction temperature was set as  $t=0$ . The conversions of *n*-butyraldehyde at different reaction times and reaction temperatures were experimentally measured and the results are listed in Table S4.

The kinetic equation is an initial-value problem of a first-order ordinary differential equation. When the initial values of the parameters  $A_+$ ,  $A_-$ ,  $Ea_+$ ,  $Ea_-$ ,  $m$  and  $n$  are given, the conversion of *n*-butyraldehyde at  $t = 3600 \text{ s}$  can be obtained by integrating the set of the first-order ordinary differential equations using a fourth-order Runge-Kutta method in the time interval of  $[0, 3600]$ . Similarly, the

conversion of *n*-butyraldehyde at  $t = i$  can be attained in the time interval of  $[0, i]$ , which is the corresponding estimated values of the reaction kinetics model. The experimental data (the conversions of *n*-butyraldehyde) at  $t = i$  were obtained by GC analyses. Then the objective function for parameter estimation is expressed as follows:

$$f = \sum_{i=1}^T \sum_{j=1}^I (x_{A,est} - x_{A,exp})^2$$

where,  $x_{A,est}$  represents the estimated conversion of *n*-butyraldehyde calculated from the model and  $x_{A,exp}$  represents the measured conversion of *n*-butyraldehyde from the experiment. The parameters can be estimated by minimizing this function using MATLAB software.

Zhang et al.<sup>41</sup> studied the kinetic of *n*-butyraldehyde self-condensation catalyzed by a sulfonic acid functionalized ionic liquids and found that both the forward and backward reactions are second order. In this study, the forward and backward reactions are supposed to be second order first and then the assumption will be verified. As a result, The estimated kinetic parameters (activation energy and pre-exponential factor of the forward and reverse reactions) are listed as follows:  $A_+ = 5.745 \times 10^5 \text{ m}^3/(\text{kmol.s})$ ;  $E_{a+} = 79.60 \text{ kJ/mol}$ ;  $A_- = 2.146 \times 10^4 \text{ m}^3/(\text{kmol.s})$ ;  $E_{a-} = 74.30 \text{ kJ/mol}$ .

### 5.2 Verification of reaction order

Substituting  $m = 2$  and  $n = 2$  to eq (7), the reaction rate equation can be expressed as follows:

$$\frac{dx_A}{dt} = k_+ C_{A0} (1 - x_A)^2 - k_- C_{A0} \left(\frac{x_A}{2}\right)^2$$

Then the above equation can be integrated to

$$\frac{1}{2\sqrt{a^2 - a}} \ln \frac{(x_A - a) - \sqrt{a^2 - a}}{(x_A - a) + \sqrt{a^2 - a}} = \frac{C_{A0}}{a} t + C$$

where  $a = \frac{k_+}{k_+ - \frac{k_-}{4}}$ ,  $C$  is the integration constant.

Suppose  $b = \frac{(x_A - a) - \sqrt{a^2 - a}}{(x_A - a) + \sqrt{a^2 - a}}$  then

$$\frac{1}{2\sqrt{a^2 - a}} \ln b = \frac{C_{A0}}{a} t + C$$

Substituting the conversion of *n*-butyraldehyde  $x_A$  determined by GC to the above equation, it is found that the relation between  $\ln b$

and  $t$  is linear, indicating that the hypothesis for second-order reaction is correct.

### 5.3 Test of kinetic model

The relationship between the experimentally measured and the estimated conversion of *n*-butyraldehyde is shown in Fig.2. It can be seen that a majority of dot are uniformly located in the both side of diagonal, demonstrating that the experimental data is well in accordance with the estimated data.

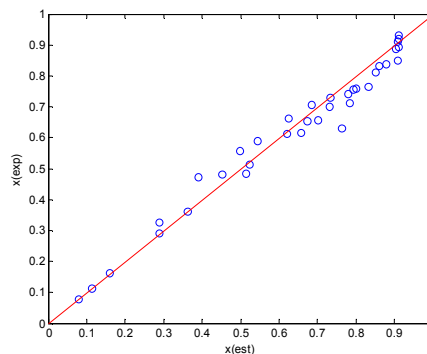


**Fig.2** Comparison between the experimental and the estimated conversion of *n*-butyraldehyde.

$x$ : conversion of *n*-butyraldehyde; est: estimated values, exp: experimental values.

The results of variation analysis and the F-test on the kinetic model are listed in Table 10. As we know from the variation analysis theory, the larger the absolute value of the correlation index and test value of  $F$ , the better the regression effect. If the correlation index  $r$  is larger than 0.9 and  $F > 10 F_{\alpha}$ , the model is considered to be suitable to the  $\alpha$  level. In this study,

$$F = \frac{\text{Re g. SS} / 3}{\text{RSS} / 31} = 349.96.$$

It can be seen that  $F$  is much bigger than  $F_{0.05}(3, 31)$  and the correlation index  $r$  is larger than 0.9. Therefore, the kinetic model is significant to the level  $\alpha = 0.05$  and thus is able to describe the *n*-butyraldehyde self-condensation reaction process.

**Table 10** Model Statistics

Experiment No.	Free variation No.	Regression squares sum	Residual squares sum	Correlation index	Variance	$F_{0.05}(3, 31)$
35	4	2.0591	0.0608	0.9856	2.0538	2.91

#### 5.4 Comparison with literature values

Lee et al.<sup>42</sup> studied the aldol condensation of *n*-butyraldehyde catalyzed by an aqueous solution of sodium hydroxide with a concentration range of 0.76 ~ 1.9 M and estimated that the activation energy was  $56.80 \pm 1.671$  kJ/mol and the pre-exponential factor was  $1.712 \times 10^8$  m<sup>3</sup>/(kmol.s) in the temperature range of 110 ~ 150 °C. Casale et al.<sup>43</sup> studied the kinetic of self-condensation of *n*-butyraldehyde catalyzed by an aqueous solution of H<sub>2</sub>SO<sub>4</sub> (85 wt %) in the temperature range of -24 ~ 42 °C and found that the activation energy and the pre-exponential factor were  $53.79 \pm 7.82$  kJ/mol and  $3.594 \times 10^8$  m<sup>3</sup>/(kmol.s), respectively. In addition, Zhang et al.<sup>41</sup> studied the kinetic of *n*-butyraldehyde self-condensation catalyzed by a sulfonic acid functionalized ionic liquid in the temperature range of 90 ~ 120 °C and obtained that the activation energy of the forward and backward reaction was separately 60.29 kJ/mol and 62.94 kJ/mol, and the corresponding pre-exponential factor was separately  $1.999 \times 10^4$  m<sup>3</sup>/(kmol.s) and  $1.001 \times 10^4$  m<sup>3</sup>/(kmol.s).

Compared with the kinetic parameters obtained from the conventional inorganic acid and base catalysts and the sulfonic acid functionalized ionic liquid, it is observed that the activation energy of the self-condensation of *n*-butyraldehyde catalyzed by Ce-Al<sub>2</sub>O<sub>3</sub> is higher, indicating that the energy barrier of such a liquid-solid phase catalytic reaction is higher and an elevated reaction temperature will be required correspondingly. Pre-exponential factor reflects the collision frequency of the reactants in a reaction system. The pre-exponential factor of this aldol condensation catalyzed by Ce-Al<sub>2</sub>O<sub>3</sub> is much less than those catalyzed by the conventional inorganic acid and base catalysts, but is equivalent to that catalyzed by the sulfonic acid functionalized ionic liquid. This is also because that the self-condensation of *n*-butyraldehyde catalyzed by Ce-Al<sub>2</sub>O<sub>3</sub> is a liquid-solid heterogeneous catalytic reaction and the resistance of mass transfer is larger, resulting in a lower pre-exponential factor.

#### Conclusions

Among a series of solid acids,  $\gamma$ -Al<sub>2</sub>O<sub>3</sub> showed a better catalytic performance for the self-condensation of *n*-butyraldehyde. The suitable preparation conditions were obtained as follows: pseudo-boehmite was calcinated at 500 °C for 4 h. Under the suitable reaction conditions of dosage of  $\gamma$ -Al<sub>2</sub>O<sub>3</sub> catalyst = 15 wt.%, reaction temperature = 180 °C and reaction time = 8 h, the conversion of *n*-butyraldehyde and the yield of 2-ethyl-2-hexenal attained 87.5% and 76.6% respectively. When  $\gamma$ -Al<sub>2</sub>O<sub>3</sub> was modified by Ce, the increase of base amount improved the selective of 2-ethyl-2-hexenal and the yield of 2-ethyl-2-hexenal could reach 83.1%. Moreover, Ce-Al<sub>2</sub>O<sub>3</sub> showed an excellent reusability. The XPS analyses of Ce3d demonstrated that the valence state of Ce affected the catalytic performance of Ce-Al<sub>2</sub>O<sub>3</sub> to some extent while the acid and base properties of Ce-Al<sub>2</sub>O<sub>3</sub> played a dominant role in its catalytic performance. Based on the analysis of the reaction system of the self-condensation of *n*-butyraldehyde catalyzed by Ce-Al<sub>2</sub>O<sub>3</sub>, some side-reactions such as the Tishchenko reaction, ketonization reaction and hydrogenation reaction were speculated and then a possible reaction network was proposed. The intrinsic kinetics for *n*-butyraldehyde self-condensation was established. Both the forward

and backward reactions are second order and the corresponding activation energy is separately 79.60 kJ/mol and 74.30 kJ/mol, higher than its homogeneous catalytic reaction system. The pre-exponential factor of the forward and backward reaction is separately  $5.745 \times 10^5$  m<sup>3</sup>/(kmol.s) and  $2.146 \times 10^4$  m<sup>3</sup>/(kmol.s), lower than the acid and base aqueous homogeneous catalytic reaction system but equivalent to the sulfonic acid functionalized ionic liquid system. The lower pre-exponential factors are due to the liquid-solid heterogeneous phase catalytic system. In conclusion, not only does Ce-Al<sub>2</sub>O<sub>3</sub> show good catalytic performance, but also it can overcome the disadvantage of the corrosion of apparatus caused by an inorganic acid or base. Therefore, Ce-Al<sub>2</sub>O<sub>3</sub> has a bright industrial prospect for the self-condensation of *n*-butyraldehyde.

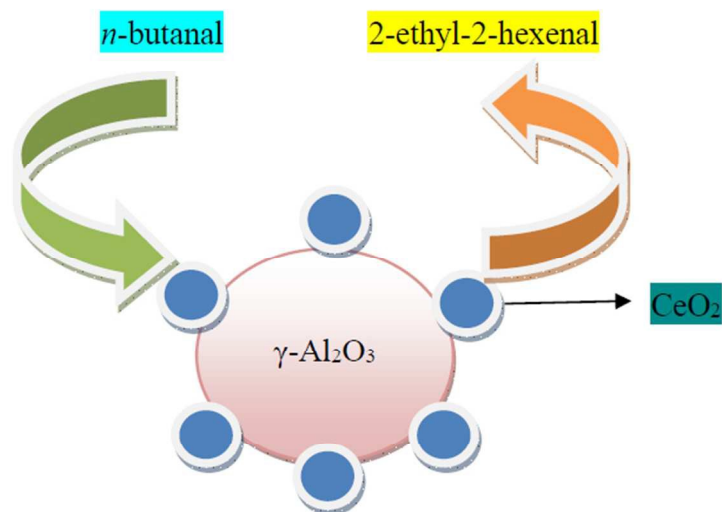
#### Acknowledgments

This work was financially supported by National Natural Science Foundation of China (Grant No. 21476058, 21236001) and Key Basic Research Project of Applied Basic Research Plan of Hebei Province (Grant No. 12965642D). The authors are gratefully appreciative of their contributions

#### Notes and references

1. S. Liu, C. Xie, S. Yu, F. Liu, Z. Song, *Ind. Eng. Chem. Res.*, 2010, **50**, 2478-2481.
2. G. J. Kelly, F. King, M. Kett, *Green Chem.*, 2002, **4**, 392-399.
3. W. Shen, G. A. Tompsett, R. Xing, W. C. Conner Jr, G. W. Huber, *J. Catal.*, 2012, **286**, 248-259.
4. F. King, G. J. Kelly, *Catal. Today.*, 2002, **73**, 75-81.
5. Y. Watanabe, K. Sawada, M. Hayash, *Green Chem.*, 2010, **12**, 384-386.
6. Y. Zhang, Thesis, Shanghai Normal University, Shanghai, China, 2010.
7. H. E. Swift, J. E. Bozik, F. E. Massoth, *J. Catal.*, 1969, **15**, 407-416.
8. N. E. Musko, J. D. Grunwaldt, *Top. Catal.*, 2011, **54**, 1115-1123.
9. C. Chen, X. Liu, H. An, X. Zhao, Y. Wang, *J. Chem. Ind. Eng.*, 2014, **65**, 2106-2112 (in Chinese).
10. O. Kikhtyanin, V. Kelbichová, D. Vitvarová, M. Kubu, D. Kubicka, *Catal. Today*, 2014, **227**, 154-162.
11. A. Lahyani, M. Chtourou, M. H. Frikha, M. Trabelsi, *Ultrason. Sonochem.*, 2013, **20**, 1296-1301
12. B. Li, R. Yan, L. Wang, Y. Diao, Z. Li, S. Zhang, *Ind. Eng. Chem. Res.*, 2014, **53**, 1386-1394.
13. J. E. Rekoske, M. A. Barteau, *Ind. Eng. Chem. Res.*, 2011, **50**, 41-51.
14. T. Komatsu, M. Mitsuhashi, T. Yashima, *Stud. Surf. Sci. Catal.*, 2002, **142**, 667-674.
15. P. Castano, G. Elordi, M. Olazar, A. T. Aguayo, B. Pawelec, J. Bilbao, *Appl. Catal. B: Environ.*, 2007, **104**, 91-100.
16. A. Ungureanu, S. Royer, T. V. Hoang, D. T. On, E. Dumitriu, S. Kaliaguine, *Microporous Mesoporous Mater.*, 2005, **24**, 283-296.

17. M. Jian, Y. Shi, D. Li, *J. Mol. Catal.*, 1990, **4**, 104-111 (in Chinese).
18. M. J. Climent, A. Corma, V. Fornés, R. Guil-Lopez, S. Iborra, *Adv. Synth. Catal.*, 2002, **344**, 1090-1096.
19. P. Huang, Z. Liu, M. Zheng, X. Xie, *Ind. Catal.*, 2003, **11**, 27-30 (in Chinese).
20. C. Anandan, P. Bera, *Appl. Surf. Sci.*, 2013, **283**, 297-303.
21. J. Z. Shyu, W. H. Weber, H. S. Gandhi, *J. Phys. Chem.*, 1988, **92**, 4964-4970.
22. F. B. Noronha, E. C. Fendley, R. R. Soares, W. E. Alvarez, D. E. Resasco, *Chem. Eng. J.*, 2001, **82**, 21-31.
23. Z. He, S. Tian, P. Ning, *J. Rare Earths.*, 2012, **30**, 563-572.
24. T. Tsoncheva, G. Issa, T. Blasco, M. Dimitrov, M. Popova, S. Hernández, D. Kovacheva, G. Atanasova, J. M. López Nieto, *Appl. Catal. A: Gen.*, 2013, **453**, 1-12.
25. V. Fernandes, I. L. Graff, J. Varald, L. Amaral, F. P. ichtner, D. Demaille, Y. Zheng, W. H. Schreiner, D. H. Mosca, *J. Electrochem. Soc.*, 2012, **159**, K27.
26. G. M. Ingo, E. Paparazzo, O. Bagnarelli, N. Zacchetti, *Surf. Interface Anal.*, 1990, **16**, 515.
27. E. Bêche, P. Charvin, P. Derarnau, S. Abanades, G. Flaman, *Surf. Interface Anal.*, 2008, **40**, 264.
28. A. Dauscher, L. Hilaire, F. L. Normand, W. Mülle, G. Maire, A. Vasquez, *Surf. Interface Anal.*, 1990, **16**, 341.
29. C. Wagner, W. Riggs, L. Davis, J. Moulder, G. Muilenberg, Perkin-Elmer corporation express, 1979, **6**, 134-135.
30. J. P. Holgado, R. Alvarez, G. Munuera, *Appl. Surf. Sci.*, 2000, **161**, 301-315.
31. V. Chauvaut, V. Albin, H. Schneider, M. Cassir, H. Ardéléan, A. Galtayries, *J. Appl. Electrochem.*, 2000, **30**, 1405.
32. N. Liang, X. Zhang, H. An, X. Zhao, Y. Wang, *Green Chem.*, 2015, **17**, 2959-2972.
33. R. Wang, Y. Guo, *Ind. Catal.*, 2015, **23**, 54-58 (in Chinese).
34. R. Bleta, P. Alphonese, L. Pin, M. Gressier, M. J. Menu, *J. Colloid Interface Sci.*, 2012, **367**, 120-128.
35. R. K. Zeidan, M. E. Davis, *J. Catal.*, 2007, **25**, 379-382.
36. H. Tsuji, F. Yagi, H. Hattori, H. Kiti, *J. Catal.*, 1994, **148**, 759-770.
37. H. Idriss, K. S. Kim, M. A. Barteau, *J. Catal.*, 1993, **139**, 119-133.
38. S. Luo, J. L. Falconer, *J. Catal.*, 1999, **185**, 393-407.
39. M. Glinski, W. Szymanski, D. Lomot, *Appl. Catal. A : Gen.*, 2005, **281**, 107-113.
40. X. Zhu, Y. Yao, H. Li, X. Lu, Sheng, Q. Sheng, *J. Chin. Rare Earth Soc.*, 2002, **20**, 468-469 (in Chinese).
41. X. Zhang, H. An, H. Zhang, X. Zhao, Y. Wang, *Ind. Eng. Chem. Res.*, 2014, **53**, 16707-16714.
42. S. Lee, A. Varma, *Chem. Eng. Sci.*, 2013, **104**, 619-629.
43. M. T. Casale, A. R. Richman, M. J. Elrod, R. M. Garland, M. R. Beaver, M. A. Tolbert, *Atmos. Environ.*, 2007, **41**, 6212-6224.



71x40mm (300 x 300 DPI)